On the magnetic coupling and spin crossover behavior in complexes containing the head-to-tail [FeII2(-SCN)2] bridging unit: A magneto-structural experimental and theoretical study

Cle Donacier Mekuimemba, Françoise Conan, Antonio J. Mota, Maria A. Palacios, Enrique Colacio, Smail Triki

On the magnetic coupling and spin crossover behavior in complexes containing the head-to-tail [$Fe^{II}_2(\mu\text{-}SCN)_2$] bridging unit: A magneto-structural experimental and theoretical study

Cle Donacier Mekuimemba,[‡] Françoise Conan,[‡] Antonio J. Mota,[†] Maria Angeles Palacios,[†] Enrique Colacio,[†]* Smail Triki[‡]*

[‡]UMR-CNRS 6521, Université de Brest (UBO), 6 Av. V. Le Gorgeu, C.S. 93837 - 29238 Brest Cedex 3, France. Email: smail.triki@univ-brest.fr

[†]Departamento de Química Inorgánica, Facultad de Ciencias, Universidad de Granada, Av. Fuentenueva S/N, 18071 Granada, Spain. Email: ecolacio@ugr.es.

ABSTRACT: A new dinuclear complex [{Fe(tpc-Obn)(NCS)(μ-NCS)}$_2$] (**1**) based on the tripodal tpc-Obn ligand (tpc-Obn = tris(2-pyridyl)benzyloxymethane), containing bridging μ-κN:κS-SCN and terminal κN-SCN thiocyanate ligands, has been prepared and characterized by single crystal X-ray diffraction, magnetic studies and DF theoretical calculations. This complex represents the first example of dinuclear Fe^{II} complex with double μ-κN:κS-SCN bridges in a head-to-tail configuration that exhibits ferromagnetic coupling between metal ions (J_{FeFe} = + 1.08 cm^{-1}). Experimental and theoretical magneto-structural studies on this kind of infrequent Fe^{II} dinuclear complexes containing a centrosymmetrically [$Fe_2(\mu\text{-}SCN)_2$] bridging fragment show that the magnitude and sign of the magnetic coupling parameter, J_{FeFe}, depend to a large extent on Fe-N-C (α) angle, so that J_{FeFe} decreases linearly when α decreases. The calculated crossover point below which the magnetic interactions change from ferromagnetic to antiferromagnetic is found at 162.3º. In addition, experimental results obtained in this work and those reported in the literature suggest that large $N_{tripodal}$-Fe^{II} distances and bent N-bound terminal κN-SCN ligands favour the high spin state of the Fe^{II} ions, while short $N_{tripodal}$-Fe^{II} distances and almost linear Fe-N-C angles favour a stronger ligand field, which enables the Fe^{II} ions to show spin crossover (SCO) behaviour.

■INTRODUCTION

Thiocyanate is a ubiquitous and versatile ligand that can exhibit a wide variety of coordination modes (see scheme 1).[1-4] Among them, κN-SCN and κS-SCN monodentate terminal and μ-κN:κS-SCN bidentate bridging (also termed end-to-end) coordination modes (a, b and c, respectively, in scheme 1) are the most commonly observed. The nitrogen and sulphur ends of this ambidentate ligand are hard and soft type bases, respectively.[5] Therefore, thiocyanate generally coordinates to the hard and soft acid metal ions through the N and S atoms, respectively.

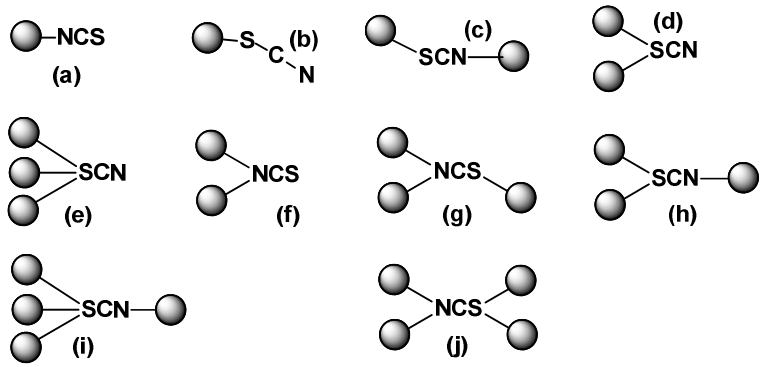

Scheme 1. Coordination modes of the thiocyanate anion. Grey balls represent metal atoms.

In line with this, thiocyanate is bound to the first row transition metal ions through the N atom, whereas the coordination to heavier transition metal ions in low oxidation state, usually takes place through the S atom. Nevertheless, in addition to the electronic nature and oxidation state of the metal ion, other factors such as steric hindrance, electronic structure of the ancillary ligands, type of solvent and even non-coordinated ions can influence the final coordination mode of the thiocyanato ligand, particularly when the metal ion has intermediate hard-soft acid character.[6] It should be noted that N-bound thiocyanate generally is linear, whereas the S-bound thiocyanato is commonly bent at the sulphur atom. The S-bound thiocyanato occupies more space that the N-bound form, so that when bulk ligands are present the latter might be favoured to avoid steric hindrance.[7,8] Although thiocyanate complexes are often a mixture of non-separable N-bound and S-bound linkage isomers,[9] however, recently the N-bound and S-bound thiocyanate linkage isomers of the [Ru(terpy)(tbbpy)SCN][SbF_6] complex

(terpy = 2,2′,6′,2″-terpyridine, tbbpy = 4,4′-di-tert-butyl-2,2′-bipyridine), could be separated based on their relative solubility in ethanol and their respective structures solved by X-ray crystallography.[10]

It is worth mentioning that N-bound thiocyanate have played an important role in the field of spin crossover (SCO) materials, which are switchable systems that exhibit reversible spin conversion between the low-spin and the high-spin states by external stimuli, such as temperature, light irradiation and pressure.[11-17] These switchable materials have potential applications in different fields, such sensors, data processing and storage, molecular switches, signal amplification and visualization devices.[11-17] Most of the SCO systems are $Fe^{II}N_6$ mononuclear species and, among them, $[Fe(L)_2(\kappa N\text{-}NCS)_2]$ type complexes (where L is a bidentate α-diimine ligand) are the most extensively studied.[11-17] In these systems, thiocyanate ligands adjust the ligand field around Fe^{II} metal ion, so that the SCO phenomenon can be observed.

When the thiocyanate anion links two or more metal ions (modes c-j in Scheme 1) a great variety of coordination networks can be obtained, which exhibit aesthetically pleasing structures and interesting physical properties. When metal ions are paramagnetic, the thiocyanato bridging ligand can transmit ferromagnetic and antiferromagnetic interactions leading to materials with interesting cooperative magnetic properties, such as ferromagnetic and antiferromagnetic long range magnetic order, metamagnetism, spin canting and single-chain magnet behaviour.[18-31] It should be noted that compared to the azido-bridged complexes, the number of well magneto-structurally characterized thiocyanate-bridged compounds with divalent first-row transition metals is very limited, particularly those containing the Fe^{II} metal ion.[28-35] Most part of these uncommon complexes present either dinuclear or chain structures with double μ-κN:κS-SCN bridged $[Fe_2(\mu\text{-}SCN)_2]$ subunits and, with a sole exception,[30] exhibit ferromagnetic interactions between the Fe^{II} ions. A simple way to study magnetic coupling through this kind of double μ-κN:κS-SCN bidentate bridges is to use dinuclear complexes. As far as we know, only two examples of $[Fe_2(\mu\text{-}SCN)_2]$ complexes have been reported so far. One of them, $[\{Fe(py_3COH)(NCS)(\mu\text{-}NCS)\}_2](PrOH)_2$[36] exhibits SCO behaviour with $T_{1/2}$ = 207 K and therefore the magnetic coupling between the Fe^{II} cannot be extracted from magnetic data. The other one, $[\{Fe(TMTAC)(NCS)_2\}_2]$[37] (TMTAC = N,N',N''-trimethyl-1,4,7-triazacyclononane) is a high spin complex that does not show SCO above 100 K. The magnetic coupling for

this compound could not be accurately analyzed because the magnetic properties were measured in the 300-100 K range.[37] More examples of head-to-tail double μ-κN:κS-SCN bidentate bridged dinuclear Fe^{2+} complexes are needed not only to establish correlations between the magnetic coupling and the structural parameters, but also to compare the structural features of HS and LS complexes and thus to try to shed light on the SCO behaviour of this type of compounds.

In this paper, we report the synthesis, crystal structure, magnetic properties and DF theoretical calculations of the high spin [{Fe(tpc-Obn)(NCS)(μ-NCS)}$_2$] (tpc-Obn = tris(2-pyridyl)benzyloxymethane) complex (**1**). The aim of this work is twofold: (i) to disclose the electronic and structural factors leading to a HS configuration in this complex and, however, to SCO behaviour in the closely structural related complex [{Fe(py_3COH)(NCS)(μ-NCS)}$_2$](PrOH)$_2$; (ii) to extract the magnetic coupling constant, *J*, for **1** and to analyze experimentally and theoretically the structural factors governing the magnitude and sign of the magnetic coupling in this kind of double μ-κN:κS-SCN bridged Fe^{II} complexes. For it, the dinuclear HS complex [{Fe(TMTAC)$(NCS)_2$}$_2$] has been prepared[37] and its magnetic data have been re-measured in the temperature range 2-300 K. In doing so, we will have on hand valuable information to design μ-κN:κS-SCN bidentate bridged Fe^{II} complexes with predictable magnetic properties.

■ RESULTS AND DISCUSSIONS.

Synthesis. The tris(2-pyridyl)benzyloxymethane (tpc-Obn) ligand was synthesized according to the previously described the method[38] (see Figures S1, S2 and S3). Complex [{Fe(tpc-OBn)(NCS)(μ-NCS)}$_2$] (**1**) was prepared by reaction of methanolic solution containing $FeCl_2.4H_2O$ and KNCS with an acetonitrile solution of the tpc-Obn ligand in a 1:2:1 molar ratio, for Fe(II), NCS- and tpc-Obn, respectively. Single yellow crystals of **1** were obtained by slow evaporation of the resulting solution at room temperature. The infrared spectrum of **1** (see Figure S4) shows two absorption bands at 2110(s) and 2055(m) cm^{-1} which can be attributed to the pseudosymmetric stretching vibration modes (ν(CN)) of the thiocyanate groups. The first one can be assigned to the bridging coordination mode of the NCS^- groups, whereas the second one can be assigned to the terminal κN-SCN coordination mode.[4]

Description of the crystal structure. Compound **1** crystallizes in the monoclinic $P2_1/c$ space group. Crystallographic data including refinement parameters,

bond lengths and bond angles are given in Tables S1-S3, respectively. The crystal structure of **1** is built from one Fe(II) ion (Fe1), one tpc-Obn and two NCS^- ligands, all located on general positions. The molecular structure of **1** consists of well isolated neutral dinuclear [{Fe(tpc-Obn)(NCS)(μ-NCS)}$_2$] molecules with C_i symmetry, the centre of symmetry being located at the middle of the line connecting the two Fe^{II} ions (Figure 1).

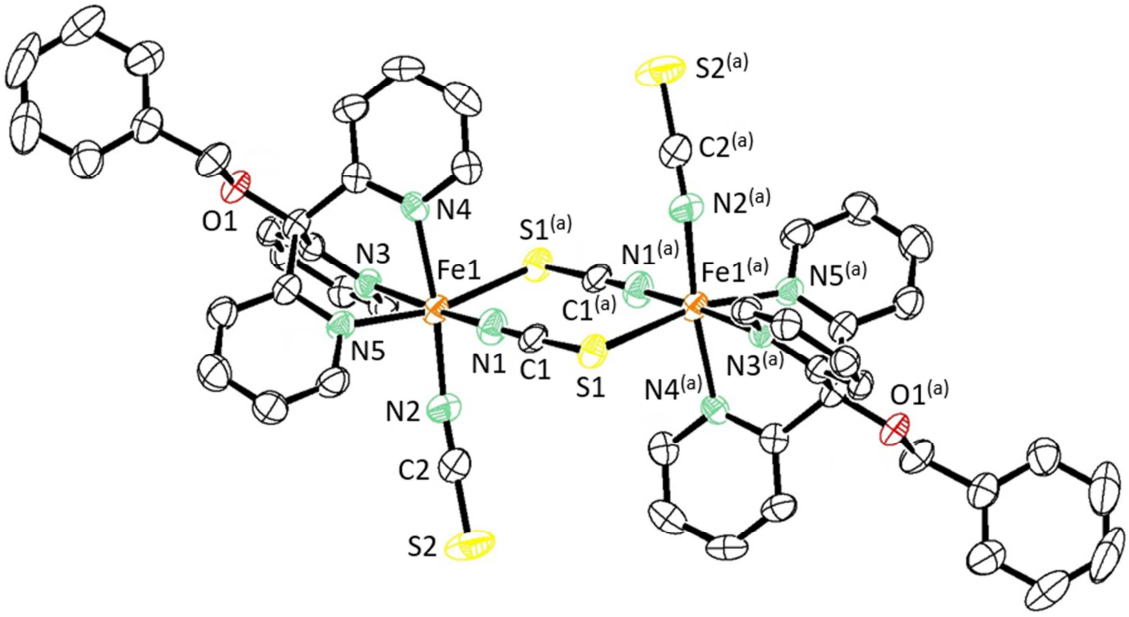

Figure 1. Perspective ORTEP view of the structure of **1**. Hydrogen atoms are omitted for the sake of clarity. Codes of equivalent position: (a) = -x,-y,-z.

Selected bond-lengths and angles are gathered in Table 1. Within the dinuclear unit, Fe^{II} atoms exhibits a slightly distorted octahedral FeN_5S coordination polyhedron, where the three pyridine nitrogen atoms of the tpc-Obn tripodal ligand, and consequently the two nitrogen atoms and the sulphur atom belonging to the end-to-end bridging and terminal thiocyanato ligands, occupy *fac* positions.

Table 1. Selected bond lengths (Å) and bond angles (°) for **1** at 170 K

Fe1-N1	2.108(4)	C1-N1	1.156(5)
Fe1-N2	2.054(4)	C1-S1	1.645(5)
Fe1-N3	2.237(3)	C2-N2	1.164(5)
Fe1-N4	2.165(3)	C2-S2	1.619(5)
Fe1-N5	2.173(3)	Fe1…Fe1$^{(a)}$	5.604(1)
Fe1-S1$^{(a)}$	2.6054(13)		
N2-Fe1-N1	94.09(15)	N2-Fe1-S1$^{(a)}$	95.37(11)
N2-Fe1-N4	173.42(14)	N1-Fe1-S1$^{(a)}$	95.16(10)
N1-Fe1-N4	90.55(14)	N4-Fe1-S1$^{(a)}$	88.84(9)
N2-Fe1-N5	95.11(14)	N5-Fe1-S1$^{(a)}$	167.00(9)
N1-Fe1-N5	91.75(13)	N3-Fe1-S1$^{(a)}$	88.54(9)
N4-Fe1-N5	80.07(12)	N1-C1-S1	177.9(4)

N2-Fe1-N3	91.49(14)	N2-C2-S2	178.3(4)
N1-Fe1-N3	172.98(13)	C2-N2-Fe1	156.6(4)
N4-Fe1-N3	83.55(12)	C1-S1-Fe1[(a)]	97.76(15)
N5-Fe1-N3	83.52(12)	C1-N1-Fe1	166.4(3)

Codes of equivalent position: (a) = -x,-y,-z.

The calculation of the degree of distortion of the Fe^{II} coordination polyhedron with respect to ideal six-vertex polyhedra, by using the continuous shape measure theory and SHAPE software,[39-40] led to shape measures relative to the octahedron (OC-6) and trigonal prism (TPR-6) with values of 0.89 and 16.17, respectively (see Table S4), the shape measures relative to other reference polyhedra being significantly larger. Therefore, the FeN_5S coordination sphere is very close to ideal OC-6. The Fe-Npyr distances are in the 2.165-2.237Å range, whereas the Fe-N distances corresponding to the terminal (Fe1-N2) and end-to-end bridging thiocyanato (Fe1-N1) ligands (2.054(4) and 2.108(4) Å, respectively) are considerably shorter. The Fe-S is the longer distance around Fe^{II} atom with a value of 2.605(2) Å. The Fe^{II} are linked by a pair of end-to-end thiocyanato bridges (μ-κN:κS-SCN coordination mode), which adopt a crystallographically imposed head-to-tail configuration. The $[Fe_2(\mu\text{-}SCN)_2]$ fragment is almost planar and, as usual, adopts a quasi-rectangular configuration with Fe-N-C and Fe-S-C angles are 166.4(3) and 97.8(2)º, respectively. The κN-bound terminal thiocyanate group is far from being linear with a Fe-N-C angle of 156.6(4)º. The intradinucler Fe···Fe distance is 5.604(1) Å, whereas the shortest Fe···Fe interdinuclear distance is 8.963(1) Å. Distances and angles around Fe^{II} ion are very similar to those observed for the closely structural related complex $[\{Fe(py_3COH)(NCS)(\mu\text{-}NCS)\}_2](PrOH)_2$ at 296 K with a HS configuration and involving a nearly similar tripodal ligand.[36] Although in the $[\{Fe(TMTAC)(NCS)_2\}_2]$ complex[37] the Fe-S and Fe-N distances belonging to the terminal an bridging thiocyanato ligands are similar to those found in **1**; however, the Fe-N distances involving the amino groups of the TMTAC ligands (2.25-2.27 Å) are significantly larger than the Fe-Npyr distances (2.165-2.237 Å). Finally, the structure does not show classical hydrogen bond interactions but weak C-H···S interactions involving the hydrogen atoms of the pyridine rings and the sulphur atoms of the terminal and bridging thiocyanato ligands.

Magnetic properties. The temperature dependence of the $\chi_M T$ product for compound **1** in the 10-300 K temperature range (χ_M being the molar magnetic susceptibility per two Fe^{II} ions) under a constant magnetic field of 0.1 T is displayed in

Figure 2. At room temperature the $\chi_M T$ value for complex **1** is 6.68 $cm^3 \cdot K \cdot mol^{-1}$, which agrees well with the expected value for two non-interacting high spin (S = 2) Fe^{II} ions with g = 2.11.[17,36,37] On cooling, the $\chi_M T$ value remains constant until approximately 50 K and then sharply increases reaching a value of 8.53 $cm^3 \cdot K \cdot mol^{-1}$ at 6 K. This latter value is lower than that calculated for an S = 4 ground state (11.13 $cm^3 \cdot K \cdot mol^{-1}$ with g = 2.11) but close to that expected for two ferromagnetically coupled Fe(II) centers with single-ion anisotropy (see below). This behavior clearly indicates the existence of a weak ferromagnetic interactions between the Fe^{II} ions through the double end-to-end thiocyanate bridge.

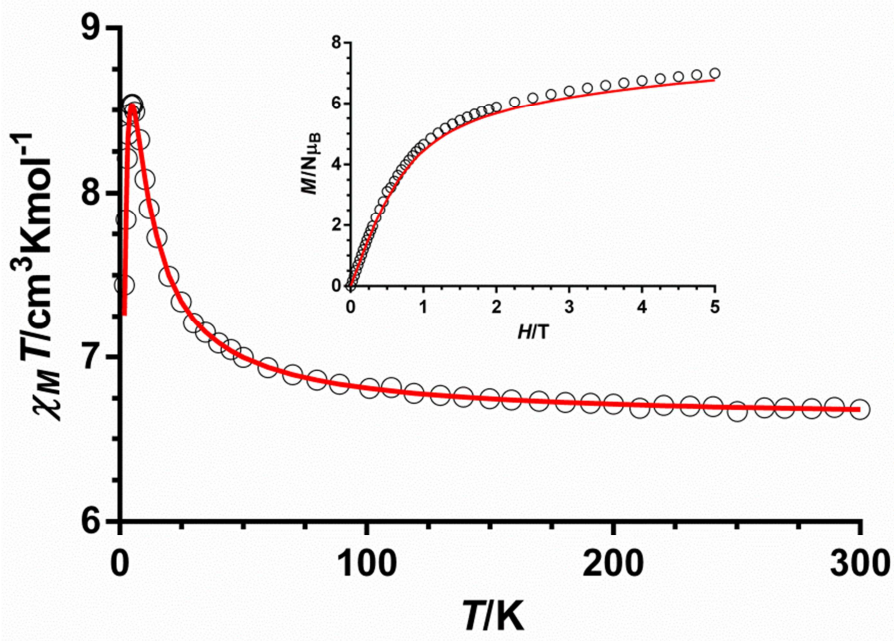

Figure 2. Temperature dependence of the $\chi_M T$ and filed dependence of magnetization for **1**. The red solid lines represent the best fit with the magnetic parameters indicated in equation (1).

In order to analyze the magnetic data, we have used the following Hamiltonian:

$$H = -J(S_{Fe1}S_{Fe2}) + \sum_{i=1}^{2} D_{Fe}S_{Fez}^2 + g\mu_B(S_{Fe1} + S_{Fe1})H \qquad (1)$$

where the first term accounts for the isotropic magnetic exchange coupling between the Fe^{II} ions, D_{Fe} is the axial single ion zero field splitting parameter and the third term corresponds to the Zeeman interaction (D_{Fe} and g are equal for both Fe^{II} atoms as they are related by a centre of symmetry). The susceptibility and magnetization was simultaneously fitted to the above Hamiltonian using the PHI[41] software to afford the following set of parameters, J = + 1.08 cm^{-1}, g = 2.10 and D = 4.3 cm^{-1} with R = 7.3x10^{-7} (R = $\{\Sigma[(\chi_M T)_{exp.}-(\chi_M T)_{calcd.}]^2/\Sigma(\chi_M T)_{exp})^2\}$. The D value is lower but still close to that

observed for other hexacoordinated Fe(II) complexes.[42] Finally, it should be noted that ac susceptibility measurements indicate that this compound does not show slow relaxation of the magnetization and SMM behaviour. This could be due to the fact that *D* is positive.

Magneto-structural relationships. In order to support the experimental value of J_{FeFe} in **1**, DFT calculations were carried out on the X-ray structure as found in solid state. The calculated J_{FeFe} parameter (+1.84 cm^{-1}) agrees in sign with the experimental parameter, but almost twice its magnitude. The difference between experimental and calculated J_{FeFe} values are most likely due, among other reasons, to limitations inherent to the theoretical method, certain inaccuracy of the magnetic data, and the possible slight changes in the structure at low temperature with regard to that used in the theoretical calculations. The calculated spin density for the S = 4 ground state of **1** is given in Figure 3 and offers information on the mechanism of the magnetic exchange interactions. The spin density distribution suggests that the main mechanism for the exchange is spin delocalization.

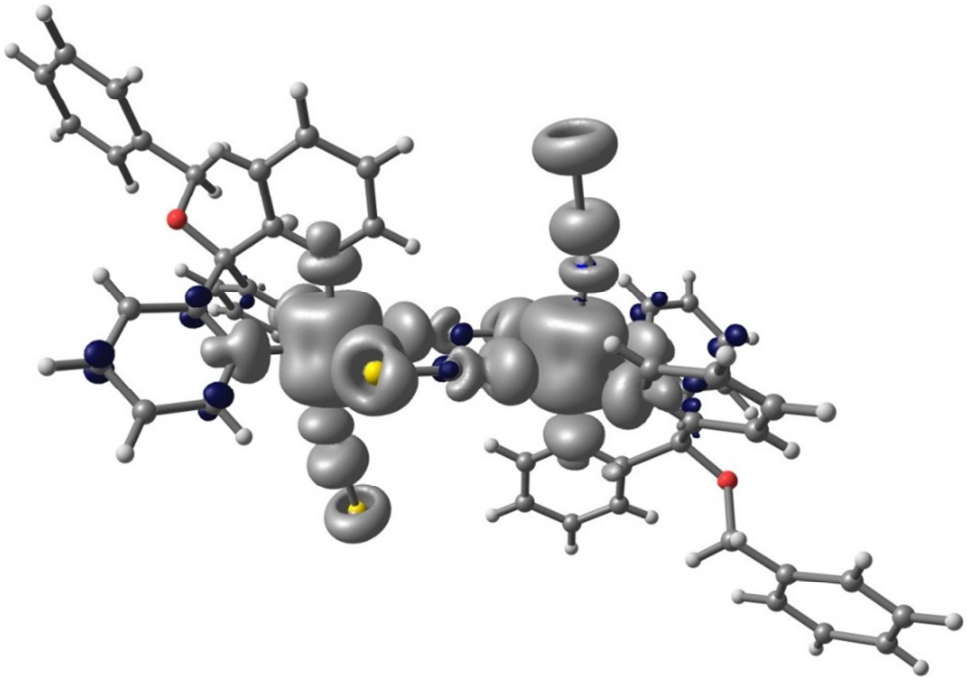

Figure 3. Spin density map (contour value of 0.001 e^{-} $Bohr^{-3}$.) for **1**. Grey and dark blue shapes correspond to positive and negative values, respectively.

The shape of the spin density of the Fe(II) ion is prismatic as expected for four unpaired electrons in five d orbitals. The flattened surfaces lie in the directions of the metal–ligand bonds and small spin densities of the same sign appear on the atoms of the ligands directly attached to the Fe^{II} centre. It should be noted that the whole spin density

is mainly located on the metallic centers (average value +3.7446 e-), whereas the atoms coordinated to the Fe(II) ions have small spin densities (< 0.047 e-) of the same sign as the Fe^{II} ion (see Table 2). The largest spin densities for these atoms are found on to the sulphur and nitrogen atoms belonging to the bridging thiocyanate group and on the pyridine nitrogen atom *trans* to the nitrogen atom of the bridging thiocyanate group. This spin distribution reveals that there is significant spin delocalization on the thiocyanate bridging group which favours the magnetic exchange interactions. The fact that the spin density of the sulphur atom belonging to the bridging thiocyanate group is mainly found on a *p* orbital perpendicular to the direction of the N *p* orbital of the same thiocyanate bridging group could explain the ferromagnetic interactions observed for this compound. In addition to the spin delocalization mechanism, it seems that the spin polarization mechanism leading to ferromagnetic interactions could be also operative as the atoms on the thiocyanate bridging group display an alternating sign of the spin densities (see Table 2).

Table 2. Spin density (in electrons) of selected atoms for **1**. Just a half of the structure is presented due to its internal C_i symmetry.

Atom(s)	Spin density
Fe	+3.7446
$N_{py\text{-}anti}$ [a]	+0.0220
N_{py} [b]	+0.0366
NCS_{bridge}	+0.0426 (N), −0.0107 (C), +0.0468 (S)
NCS_{ax}	+0.0131 (N), +0.0242 (C), +0.0440 (S)

[a]The pyridinic nitrogen that is located in *anti* position with respect to the nitrogen atom of the SCN bridging ligand. [b]For the rest of the pyridinic nitrogen atoms mean values are given.

Let us to comment about the values and nature of the magnetic exchange interactions in Fe^{II} complexes containing double bridged head-to-tail $[Fe_2(\mu\text{-}SCN)_2]$ dinuclear subunits. First, we are going to compare the structural and magnetic properties of this type of complexes to determine the structural parameters governing the sign and strength of the magnetic exchange interactions. As **1** is the only example of a fully magneto-structural characterized head-to-tail $[Fe_2(\mu\text{-}SCN)_2]$ dinuclear complex, we have included the limited existing data for 1D chain complexes where the two Fe-S_{bridge}, and consequently the two Fe-N_{bridge}, occupy *trans* positions on the Fe^{II} coordination sphere.

Table 3. Experimental magneto-structural data for dinuclear and chain complexes containing the $[Fe_2(\mu\text{-}SCN)_2]$ fragment

Compound	J (cm^{-1})	Fe-N-C_{bridge}	Fe-S-C_{bridge}	Ref.

[{Fe(tpc-Obn)(NCS)(μ-NCS)}$_2$] **1**	+1.08	166.4	97.8	t.w.
[{Fe(TMTAC)(NCS)$_2$}$_2$]	-4.0	156.1	101.2	37, t.w.
[{Fe(py$_3$COH)(NCS)(μ-NCS)}$_2$](PrOH)$_2$	[a]	164.81[b]	100.67[b]	36
[f][Fe(NCS)$_2$(bpe)$_2$]$_n$	+0.90	164.50[c]	100.70[c]	31
[f][Fe(NCS)$_2$(py)$_2$]$_n$	F[d]	165.35 [c]	99.42[c]	29
[f][Fe(NCS)$_2$TCNQ]$_n$	AF[d]	153.07	101.45	30
[Fe(NCS)$_2$(OCMe$_2$)$_2$]$_n$	+1.2	165.45	101.75	28

[a]spin crossover transition. [b]high spin configuration at 300 K [c]Average values. [d]The magnetic coupling was not quantitatively extracted. [f]bpe = 1,2-bis(4-pyridyl)ethene, py = pyridine, TCNQ = 7,7,8,8-tetracyano-p-quinodimethane. t.w. = this work

In the two remaining *trans* positions are located either two nitrogen or two oxygen atoms belonging to the ancillary ligands. Selected magneto-structural data for this type of complexes are given in Table 3. As it can be observed in this table, the magnetic coupling between the Fe^{II} atoms through the double end-to-end bridge is ferromagnetic, except for one case. Moreover, large Fe-N-C and small Fe-S-C angles favour ferromagnetic interactions with the crossing point between F and AF interactions at a Fe-N-C angle in the range 153º-164º. The lack of enough experimental data in this region precludes an accurate determination of the crossing point. It should be noted that a similar trend has been proposed from experimental data and semiempirical extended Hückel calculations for double end-to-end dinuclear Ni^{II} complexes, which, at variance with the Fe^{II} complexes, in all cases exhibit ferromagnetic interactions.[43] Moreover, it seems that the deviation of the Fe^{II} atoms from the plane of the [Fe_2(μ-SCN)$_2$] dinuclear bridging units could also affect the magnetic interactions. Thus, all the structures exhibiting ferromagnetic interactions contain almost planar [Fe_2(μ-SCN)$_2$] dinuclear bridging units with maximum deviation of the Fe^{II} from the FeNSFeSN mean plane < 0.05 Å, whereas that displaying AF interactions, [Fe(NCS)$_2$TCNQ],[30] has a chair-like conformation of the [Fe_2(μ-SCN)$_2$] dinuclear bridging unit with a significant deviation of the Fe^{II} ion with respect to the FeNSFeSN mean plane of 0.21 Å. Noteworthy, this larger deviation also corresponds to the compounds containing the lowest Fe-N-C angles (< 157º), for which AF interactions are expected. We have carried out DFT calculations on different head-to-tail [Fe_2(μ-SCN)$_2$] dinuclear model complexes to support the experimental magneto-structural correlation and to quantitatively evaluate the variation of *J* with the Fe-N-C and Fe-S-C angles and with the deviation from the planarity of the [Fe_2(μ-SCN)$_2$] bridging fragment toward a chair-like geometry. Firstly, we have replaced the pyridyl moieties of the tpc-Obn ligands by imine groups and the phenyl ring by a methyl group, all other structural parameters being the same as in **1** (Figure 4). The calculated J_{FeFe} value for this model of +1.42 cm^{-1} points out that these

structural changes do not affect in a large extent the magnitude of $J_{FeFe.}$. Secondly, the terminal thiocyanato ligands of this model were changed from a bent to a linear conformation. However, this change does not alter the value of J_{FeFe}. Thirdly, terminal thiocyanato ligands were replaced by ammonia molecules. In this case, the J_{FeFe} decreases to a value of +1.15 cm^{-1}. In view of the above results, it seems that none of these changes produce large modifications of the J_{FeFe} with respect to that calculated for **1** as to explain the existence of antiferromagnetic interactions in $[Fe(NCS)_2TCNQ]$. Therefore, other structural factors must affect the J_{FeFe} value in a larger extent. In view of this and in agreement with the experimental observed magneto-structural correlation for these head-to-tail $[Fe_2(\mu\text{-}SCN)_2]$ complexes (Table 3), which indicates that J_{FeFe} increases with increasing the Fe-N-C angle in the bridging region (α), we have performed the following calculations on the model complex in Figure 4: (i) the bridging fragment was forced to be planar and the α angle was varied in the 166.37º (the value for this angle in **1**)-132.4º range (the decrease in α produces a simultaneous increase of both the Fe-S-C angle and the Fe···Fe intradinuclear distance).

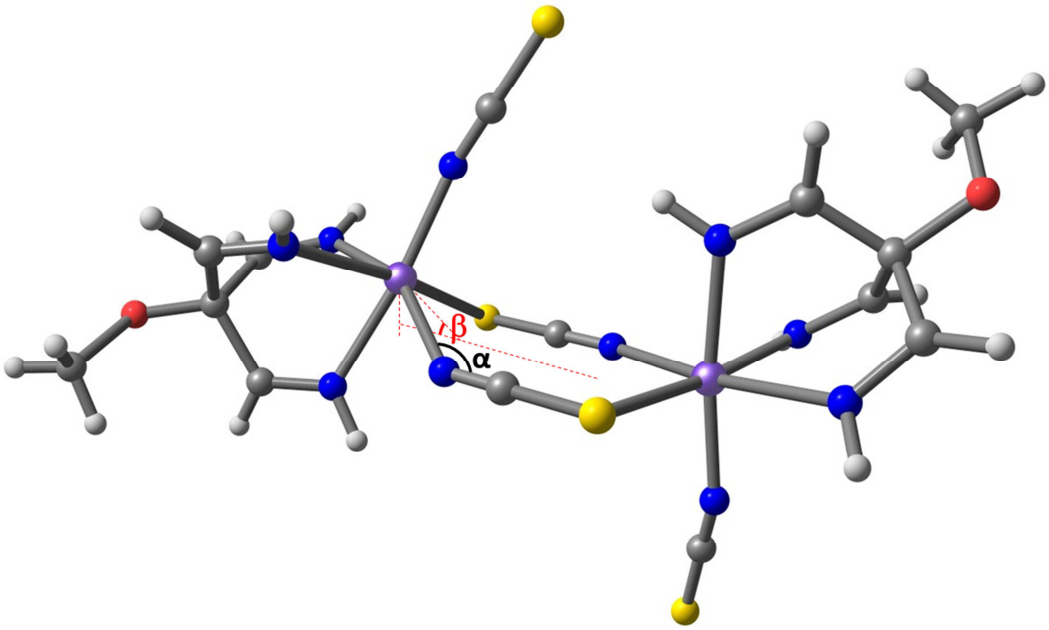

Figure 4. Model compound used for DFT calculations.

The DFT results (see Figure 5) clearly show that (i) J_{FeFe} depends to a large extent on α and confirm that J_{FeFe} decreases linearly when α decreases, so that for α values lower than 162.3º (the crossover point below which the magnetic interactions change from ferromagnetic to antiferromagnetic) the magnetic exchange interaction J_{FeFe} is expected to be antiferromagnetic, reaching a value of -15.2 cm^{-1} at 132º. It is worth mentioning

that a small decrease in α of about 4º is able to pass from the larger ferromagnetic interactions to an antiferromagnetic coupling; (ii) The α angle was fixed to 166.4º (Figure 5) and then the dihedral β angle (angle between the NSNS plane in the bridging region and the plane formed by the iron atom and the N and S atoms of the thiocyanato bridging ligands connected to it) was varied from zero (planar bridging fragment) to 30°. In doing so, the Fe^{II} ion deviates from the NSNS plane and the planar bridging fragment changes toward a chair-like conformation (Figure 5). The larger the β angle is, the larger the deviation of the Fe^{II} atom. The results clearly indicate that J_{FeFe} decreases with β and that this structural factor has a less influence on the value of J_{FeFe} than the α angle. Thus a variation of β of 30º only produces a total variation of J_{FeFe} of about 1 cm^{-1}, whereas a similar change of α produces a much larger variation of J_{FeFe} (approximately 15 cm^{-1}). Therefore, it is clear that the main factor controlling the sign and magnitude of J_{FeFe} is the Fe-N-C (α) angle.

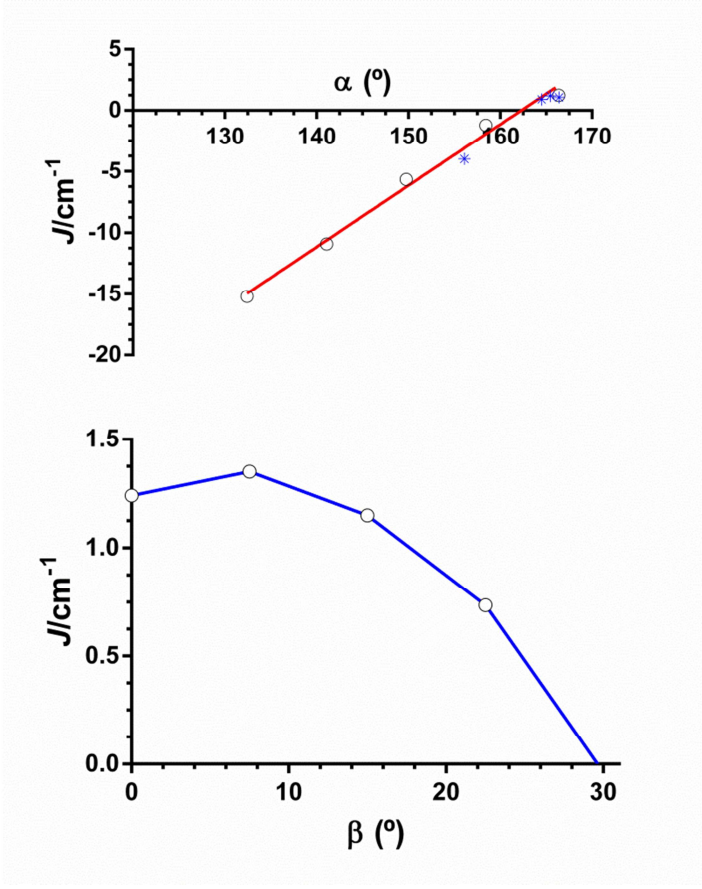

Figure 5. (Top) Dependence of the theoretically calculated J_{FeFe} values with α for β fixed to 0° (circles). The red solid line represents the best linear fit of the calculated J_{FeFe} values. The asterisk symbols represent the experimental *J* values included in Table

3. (Bottom) Dependence of the theoretically calculated *J* values with β with the α angle fixed to 166.4°. The blue solid line is only a guide for the eye.

Taking into account the above theoretical and experimental magneto-structural correlations for dinuclear complexes containing a centrosymmetrically [$Fe_2(\mu\text{-}SCN)_2$] bridging fragment, the dinuclear complex [{$Fe(TMTAC)(NCS)_2$}$_2$][37] is expected to exhibit a weak antiferromagnetic coupling between the Fe^{II} atoms. To support this, we have synthesized the complex [{$Fe(TMTAC)(NCS)_2$}$_2$] and we have re-measured its magnetic properties between 2-300 K (Figure 6).

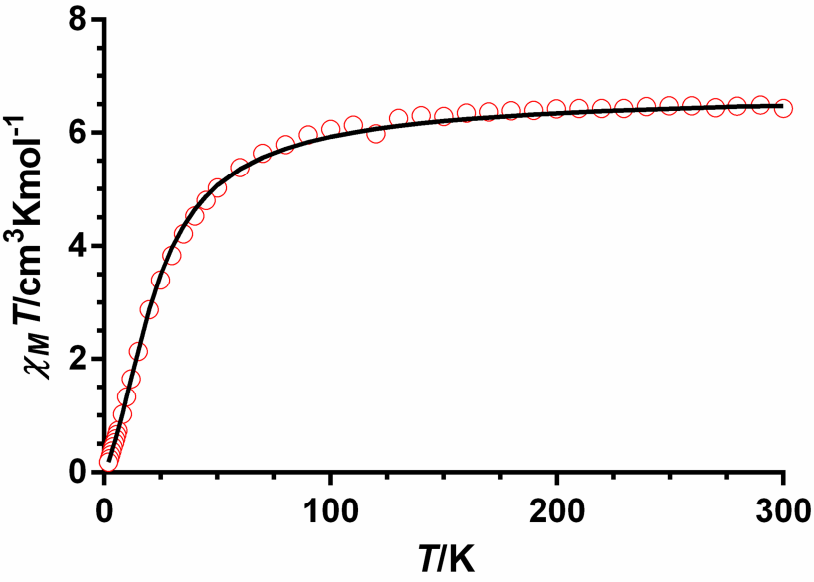

Figure 6. Temperature dependence $\chi_M T$ for [{$Fe(TMTAC)(NCS)_2$}$_2$] (TMTAC = N,N',N''-trimethyl-1,4,7-triazacyclononane). This neutral dinuclear complex has been prepared according to the reference 37. The red solid lines represent the best fit with the magnetic parameters indicated in the eq.1.

The room temperature $\chi_M T$ value of 6.47 $cm^3 \cdot K \cdot mol^{-1}$, is compatible with two non-interacting HS Fe^{II} ions (S = 2) with g = 2.08. On lowering temperature, the $\chi_M T$ value slowly decreases until approximately 50 K and then sharply reaching a value of 0.18 $cm^3 \cdot K \cdot mol^{-1}$ at 2 K. This behavior points out the existence of weak antiferromagnetic interactions between the Fe^{II} ions through the double end-to-end thiocyanate bridge. The analysis of the magnetic data with the Hamiltonian in eq.1 afforded the following magnetic parameters: J = - 4.0 cm^{-1} and g = 2.12 and D = 9.20 cm^{-1} with R = 9 x10^{-6}. The expected value using the theoretical J vs (α) magneto-structural correlation is -3.15 cm^{-1}, which is close to that extracted from experimental magnetic data. The

experimental and theoretical *J* values (Table 3 and Figure 5) confirm the goodness of the above magneto-structural correlation and therefore it can be used for quantitative predictions. When the structures for the HS configurations of the dinuclear compounds (compound **1**, $[\{Fe(py_3COH)(NCS)(\mu\text{-}NCS)\}_2](PrOH)_2$[36] and $[\{Fe(TMTAC)(NCS)_2\}_2]$[37]) are compared, the following conclusions can be drawn: (i) the Fe-N distances involving the amine and terminal thiocyanato nitrogen atoms for $[\{Fe(TMTAC)(NCS)_2\}_2]$ are rather larger than those for **1** and $[\{Fe(py_3COH)(NCS)(\mu\text{-}NCS)\}_2](PrOH)_2$. This fact leads to a lower ligand field around Fe^{II} in $[\{Fe(TMTAC)(NCS)_2\}_2]$, thus favouring the experimentally observed HS spin configuration; (ii) Fe-X (X = S, N) distances and angles around the Fe^{II} atom, as well as the distortion of the FeN_5S octahedron, are very similar for **1** and $[\{Fe(py_3COH)(NCS)(\mu\text{-}NCS)\}_2](PrOH)_2$ at 300 K (shape measures of 0.89 and 0.87 relative to OC-6, respectively). Although the whole set of Fe-X distances is 0.044 Å larger for **1**, it does not justify why $[\{Fe(py_3COH)(NCS)(\mu\text{-}NCS)\}_2](PrOH)_2$ exhibits SCO behaviour and compound **1** does not. Nevertheless, a close examination of the structure reveals that the Fe-N-C angle for the terminal thiocyanato ligand is rather larger for $[\{Fe(py_3COH)(NCS)(\mu\text{-}NCS)\}_2](PrOH)_2$ (171.05º) than for **1** and $[\{Fe(TMTAC)(NCS)_2\}_2]$ displaying similar angle (156.6º). In these two latter complexes the steric hindrance from the tripodal ligand (with weak intra and intermolecular S···H-C interactions) could lead to a bent conformation of the N-bound terminal thiocyanato ligand. In $[\{Fe(py_3COH)(NCS)(\mu\text{-}NCS)\}_2](PrOH)_2$, however, the steric hindrance effect is overcome by the short hydrogen bond involving the sulphur atom of terminal thiocyanato ligand and the oxygen atom of the propanol crystal molecule, leading to an almost lineal thiocyanato ligand.

It should be noted at this point that ligand-field analyses carried out on the complexes $[Ni(en)_2(SCN)_2]$ and $[Ni(NH_3)_4(SCN)_2]$ using the angular overlap model (AOM) studies[44] have shown that for the bent N-bound thiocyanate in the former complex a negative parameter e_π has to be considered, whereas for the linear N-bound thiocyanate in the latter the e_π parameter is positive. Moreover, the e_σ parameter drastically decreases on passing from $[Ni(NH_3)_4(SCN)_2]$ to $[Ni(en)_2(SCN)_2]$. However, this decrease in e_σ seems to be too strong as to be only ascribed to the longer Ni-NSC bond distance in $[Ni(en)_2(SCN)_2]$, and therefore the bent N-bound thiocyanato could also contribute to this decrease. In view of the above considerations, **1** and

[{Fe(TMTAC)$(NCS)_2$}$_2$], with bent N-bound thiocyanato ligands, should exhibit weaker ligands field than [{Fe(py_3COH)(NCS)(μ-NCS)}$_2$]$(PrOH)_2$, which favours the experimentally observed HS configuration for the two former complexes. In order to confirm this hypothesis, we are now preparing similar dinuclear Fe^{II} complexes with less sterically demanding tridentate ligands, where the terminal thiocyanato ligand can adopt a linear conformation.

■ CONCLUSIONS

We have succeeding in preparing a new example of the uncommon Fe^{II} dinuclear complexes containing a centrosymmetrically $[Fe_2(\mu\text{-}SCN)_2]$ bridging fragment by reacting the tripodal tridentate tpc-Obn ligand (tpc-Obn = tris(2-pyridyl)benzyloxymethane), with $FeCl_2.4H_2O$ and KNCS in a 1:2:1 molar ratio. In this complex of formula $[Fe(tpc\text{-}Obn)(NCS)(\mu\text{-}NCS)\}_2]$ (**1**), the Fe^{II} ions are connected by a pair of end-to-end thiocyanato bridges (μ-κN:κS-SCN coordination mode) in a head-to-tail configuration, and the metal environment exhibits a slightly distorted octahedral FeN_5S coordination polyhedron involving the three pyridine nitrogen atoms of the tpc-Obn tripodal ligand in *fac* positions and the two nitrogen atoms and the sulphur atom belonging to the end-to-end bridging and terminal thiocyanato ligands, respectively. $[Fe(tpc\text{-}Obn)(NCS)(\mu\text{-}NCS)\}_2]$ is the first example of a head-to-tail double end-to-end bridged Fe^{II} dinuclear complex exhibiting ferromagnetic coupling between the metal ions (J_{FeFe} = +1.08 cm^{-1}). DFT calculations support the sign and magnitude of the experimental value. The spin distribution reveals that there is significant spin delocalization on the μ-κN:κS-SCN bridging groups and the spin density of the sulphur atoms of these bridging thiocyanate groups is mainly found on a *p* orbital perpendicular to the direction of the N *p* orbital of the same thiocyanate bridging group, which could support the presence of ferromagnetic exchange interactions in **1**. The analysis of structural and magnetic data for the limited number of head-to-tail double end-to-end bridged Fe^{II} dinuclear and chain complexes allows establishing that large Fe-N-C and small Fe-S-C angles in the $[Fe_2(\mu\text{-}SCN)_2]$ bridging fragment favour ferromagnetic interactions with the crossover point between F and AF interactions at a Fe-N-C angle in the range 153º-164º. Moreover, the deviation of the Fe^{II} atoms from the plane of the $[Fe_2(\mu\text{-}SCN)_2]$ dinuclear bridging units seems also to affect the magnetic interaction. DFT calculations on a $[Fe_2(\mu\text{-}SCN)_2]$ dinuclear model complex support the experimental magneto-structural correlation, as they show that J_{FeFe} decreases linearly when α (the Fe-N-C angle) decreases, so that the crossover point between F and AF interactions is found at $\alpha = 162.3º$ for a planar $[Fe_2(\mu\text{-}SCN)_2]$ fragment. Although the change from planar toward a chair-like conformation of this bridging fragment, with the concomitant deviation of the Fe^{II} atoms from the FeNSFeSN mean plane, also declines J_{FeFe}, however, it is clear from DFT calculations that the main factor controlling the sign

and magnitude of J_{FeFe} is the α angle. Interestingly, these magneto-structural correlations predict antiferromagnetic interactions for the previously reported dinuclear [{Fe(TMTAC)(NCS)$_2$}$_2$] (TMTAC = N,N',N''-trimethyl-1,4,7-triazacyclononane). We have re-measured the magnetic properties of this compound and the results agree rather well with the predicted J_{FeFe} values.

Comparison of the structural parameters observed for the HS complexes [Fe(tpc-Obn)(NCS)(μ-NCS)}$_2$] and [{Fe(TMTAC)(NCS)$_2$}$_2$] and for the spin crossover (SCO) complex [{Fe(py$_3$COH)(NCS)(μ-NCS)}$_2$](PrOH)$_2$ suggests that large $N_{tripodal}$-Fe^{II} distances combined with bent N-bound terminal κN-SCN ligands lead to weak ligands field that favour the high spin state of the Fe^{II} ions for the two former complexes, while short $N_{tripodal}$-Fe^{II} distances and almost linear Fe-N-C angles promote a stronger ligand field, which enables the Fe^{II} ions in the latter complex to show spin crossover (SCO) behaviour. In order to confirm this assumption, we are now pursuing the preparation of similar dinuclear Fe^{II} complexes with less sterically demanding tridentate ligands favouring a linear conformation of the terminal thiocyanato ligand.

■ EXPERIMENTAL SECTION

General Procedures. Unless stated otherwise, all reactions were conducted in oven-dried glassware in aerobic conditions, with the reagents purchased commercially and used without further purification. The dinuclear [{Fe(TMTAC)(NCS)$_2$}$_2$] (TMTAC = N,N',N''-trimethyl-1,4,7-triazacyclononane) complex and the tris(2-pyridyl)benzyloxymethane (tpc-Obn) ligand were prepared as previously described (see Figure S1-S3).[37-38]

Preparation of [{Fe(tpc-Obn)(NCS)(μ-NCS)}$_2$] (1). Iron (II) chloride tetrahydrate $FeCl_2 \cdot 4H_2O$, (99.4 mg, 0.5 mmol) and potassium thiocyanate (97.2 mg, 1.0 mmol) were dissolved in the presence of ascorbic acid in distilled methanol (25 mL). The solution was filtered and then a solution of tris(2-pyridyl)benzyloxymethane (tpc-Obn)[38] (176.5 mg, 0.5 mmol) in acetonitrile (25 mL) was added slowly. After stirring for five minutes, the mixture was filtered again. Single yellow prismatic crystals of **1** were then formed after two days of slow evaporation at room temperature (yield. 102.5 mg, 39.0 %). Anal. Calcd. for $C_{25}H_{19}FeN_5OS_2$ (**1**): C, 57.1; N, 13.3; H, 3.6. Found: C, 56.8; N, 13.6; H, 3.5. IR data (ν/cm^{-1}) of **1** (see Figure S4): 2110(s), 2055(m), 1593(w), 1578(w), 1460(w), 1436(w), 1388(w), 1288(w), 1219(w), 1189(w), 1150(w), 1133(w), 1098(w), 1015(w),

999(w), 974(w), 931(w), 916(w), 895(w), 790(w), 771(w), 755(w), 726(m), 671(m), 660(w), 552(w), 530(w), 505(w), 479(w), 461(w), 426(w), 416(w).

Physical Measurements. Infrared (IR) spectra were collected in the range 4000−200 cm^{-1} on a FT-IR BRUKER ATR VERTEX70 Spectrometer. Elemental analyses were performed at the "Service de microanalyse", CNRS, 91198 Gif-sur-Yvette, France. ^{1}H and ^{13}C NMR spectra were recorded on Bruker AMX-300, AMX-400 and AMX-500 spectrometers, and the spectra were referenced internally using residual proton solvent resonances relative to tetramethylsilane (δ = 0 ppm). Magnetisation and variable temperature (2-300 K) magnetic susceptibility measurements on crushed single crystal samples were carried out with a Quantum Design SQUID MPMS XL-5 using a magnetic field of 0.1 T. Field dependent magnetisation measurements were carried out at different temperatures in the field range 0-5 T. The experimental susceptibilities were corrected for the diamagnetism of the constituent atoms by using Pascal's tables.

Crystallographic Data Collection and Refinement. The crystallographic study of compound **1** was performed at 170 K. The crystallographic data have been collected on an Oxford Diffraction Xcalibur CCD diffractometer with Mo Kα radiation. A single crystal of 0.21 x 0.06 x 0.05 mm^3 was used to collect the data. The data collection was performed using 1° ω-scans with an exposure time of 70 s per frame. The unit cell determination and data reduction were performed using the CrysAlis program suite on the full set of data.[45] The crystal structure was solved by direct methods and successive Fourier difference syntheses with the Sir97 program[46] and refined on F^2 by weighted anisotropic full-matrix least-square methods using the SHELXL97 program.[47] All non-hydrogen atoms were refined anisotropically while the hydrogen atoms were calculated and therefore included as isotropic fixed contributors to F_c. Due to the low absorption coefficient of **1** only semi-empirical absorption correction was needed and performed by the multi-scan method.[45] Crystallographic data including refinement parameters, and bond lengths and bond angles, and continuous shape measures calculation are given in Tables S1-S4, respectively.

Computational Details. All theoretical calculations were carried out at the density functional theory (DFT) level using the broken-symmetry approach[48] in combination with hybrid B3LYP exchange-correlation functional calculations,[49-51] as implemented in the Gaussian 09 program.[52] A quadratic convergence method was employed in the self-

consistent-field process.[53] The triple-ζ quality basis set proposed by Ahlrichs and co-workers[54] has been used for all atoms. Calculations were performed on complexes built from experimental geometries as well as on model complexes. The electronic configurations used as starting points were created using Jaguar 7.9 software.[55] The approach used to determine the exchange coupling constants for polynuclear complexes has been described in detail elsewhere.[56-59]

■ ASSOCIATED CONTENT

Supporting information

The Supporting Information is available free of charge on the ACS Publications website at DOI: 10.1021/acs.inorgchem.7b03082

X-ray crystallographic data in CIF format: CCDC number 1570854 (CIF). This material is available free of charge via the Internet at http://pubs.acs.org.

■ AUTHOR INFORMATION

Corresponding author

*E-mail: smail.triki@univ-brest.fr and ecolacio@ugr.es.

Author Contributions

The manuscript was written through contributions of all authors.

Notes

The authors declare no competing financial interest.

■ ACKNOWLEDGMENTS

The authors acknowledge the CNRS (Centre National de la Recherche Scientifique), the "Université de Brest", the "Agence Nationale de la Recherche" (ANR project BISTA-MAT: ANR-12-BS07-0030-01). EC and A.J.M thank the financial support from the Junta de Andalucía (FQM-195) and the Project of excellence P11-FQM-7756, MINECO of Spain (Project CTQ2014-56312-P) and the University of Granada. Support from the University of Granada Super-computation Centre is also acknowledged.

■ REFERENCES

(1) Bailey, R. A.; Kozak, S. L.; Michelsen T. W.; Mills, W. N. Infrared spectra of complexes of the thiocyanate and related ions. *Coord. Chem. Rev*. **1971**, *6*, 407–445.

(2) Golub, H. von A. M.; Köhler, H.; Skopenko, V. V. *in Chemistry of Pseudohalides*, Eds. Elsevier, Amsterdam,1986.

(3) Burmeister, J. Ambidentate ligands, the schizophrenics of coordination chemistry. *Coord. Chem. Rev*. **1990**, *105*, 77-133.

(4) Kabesova, M.; Gazo, J. Structure and classification of thiocyanates and the mutual influence of their ligands. *Chcm. Zvesti* **1980***, 34,* 800-841.

(5) Pearson, R. G. Hard and soft acids and bases—the evolution of a chemical concept. *Coord. Chem. Rev.* **1990**, *100*, 403–425.

(6) Vrieze K.; van Koten, G., in Comprehensive Coordination Chemistry, Pergamon, Oxford, **1987**, vol. 2, p. 225.

(7) Huheey, J. E.; Keiter, E. A.; Keiter, R. L. lnorganic Chemistry: Principles of Structure and. Reactivity, 4th ed.. Harper. Collins College Publishing: New York, **1993**.

(8) Palenik, G. J.; Clark, G. R. Crystal and molecular structure of isothiocyanatothiocyanato-(1-diphenylphosphino-3-dimethylaminopropane)palladium(II). *Inorg. Chem.* **1970**, *9*, 2754–2760.

(9) González, R.; Acosta, A.; Chiozzone, R.; Kremer, C.; Armentano, D.; De Munno, G.; Julve, M.; Lloret, F.; Faus, J. New Family of Thiocyanate-Bridged Re(IV)-SCN-M(II) (M = Ni, Co, Fe, and Mn) Heterobimetallic Compounds: Synthesis, Crystal Structure, and Magnetic Properties. *Inorg. Chem.* **2012**, *51*, 5737−5747.

(10) Brewster, T. P.; Ding, W.; Schley, N. D.; Hazari, N.; Batista, V. S.; Crabtree, R. H. Thiocyanate Linkage Isomerism in a Ruthenium Polypyridyl Complex. *Inorg. Chem.* **2011**, *50*, 11938–11946.

(11) *Spin Crossover in Transition Metal Compounds I, II, and III in Topics in Current Chemistry*; Gütlich, P.; Goodwin, H. A, Eds.; Springer-Verlag, Berlin, 2004, Vol. 233 (I), Vol. 234(II); Vol. 235 (III).

(12) Real, J. A.; Gaspar, A. B.; Niel, V.; Muñoz, M. C. Communication between iron(II) building blocks in cooperative spin transition phenomena. *Coord. Chem. Rev.* **2003**, *236*, 121-141.

(13) Real, J. A.; Gaspar, A. B.; Muñoz, M. C. Thermal, pressure and light switchable spin-crossover materials. *Dalton Trans*. **2005**, 2062-6079.

(14) Halcrow, M. A. Structure: function relationships in molecular spin-crossover complexes. *Chem. Soc. Rev.* **2011**, *40*, 4119-4142.

(15) *Spin-Crossover Materials: Properties and Applications*, Halcrow M. A, Eds.; John Wiley & Sons, Chichester, UK, 2013.

(16) Atmani, C.; El Hajj, F.; Benmansour, S.; Marchivie, M.; Triki, S.; Conan, F.; Patinec, V.; Handel, H.; Dupouy, G.; Gómez-García, C. J. Guidelines to design new spin crossover materials. *Coord. Chem. Rev*. **2010**, *254*, 1559–1569.

(17) Milin, E.; Patinec, V.; Triki, S.; Bendeif, E.-E.; Pillet, S.; Marchivie, M.; Chastanet, G.; Boukheddaden, K. Elastic Frustration Triggering Photoinduced Hidden Hysteresis and Multistability in a Two-Dimensional Photoswitchable Hofmann-Like Spin-Crossover Metal–Organic Framework. *Inorg. Chem.* **2016**, *55*, 11652–11661.

(18) Vicente, R.; Escuer, A.; Ribas, J.; Solans, X. Crystal structure and magnetic behaviour of a new kind of one-dimensional nickel(II) thiocyanate compound [{NiL(SCN)(μ-SCN)}$_n$] [L = bis(3-aminopropyl)methylamine]. *J. Chem. Soc., Dalton Trans.* **1994**, 259-262.

(19) Chattopadhyay, S.; Drew, M. G. B.; Diaz, C.; Ghosh, A. The first metamagnetic thiocyanato-bridged one-dimensional nickel(II) complex. *Dalton Trans.* **2007**, 2492–2494.

(20) Werner, J.; Rams, M.; Tomkowicz, Z.; Näther, C. A. Co(II) thiocyanato coordination polymer with 4-(3-phenylpropyl)pyridine: the influence of the co-ligand on the magnetic properties. *Dalton Trans.* **2014**, *43*, 17333−17342.

(21) Wöhlert, S.; Tomkowicz, Z.; Rams, M.; Ebbinghaus, S. G.; Fink, L.; Schmidt, M. U.; Näther, C. Influence of the Co-Ligand on the Magnetic and Relaxation Properties of Layered Co(II) Thiocyanato Coordination Polymers. *Inorg. Chem.* **2014**, *53*, 8298−8310.

(22) Werner, J.; Tomkowicz, Z.; Rams, M.; Ebbinghaus, S. G.; Neumann, T.; Näther, C. Synthesis, structure and properties of $[Co(NCS)_2(4\text{-}(4\text{-chlorobenzyl})pyridine)_2]_n$ that shows slow magnetic relaxations and a metamagnetic transition. *Dalton Trans.* **2015**, *44*, 14149−14158.

(23) Rams, M.; Tomkowicz, Z.; Böhme, M.; Plass, W.; Suckert, S.; Werner, J.; Jess, I.; Näther, C. Influence of the Metal Coordination and the Co-ligand on the Relaxation Properties of 1D $Co(NCS)_2$ Coordination Polymers. *Phys. Chem. Chem. Phys.* **2017**, *19*, 3232−3243.

(24) Boeckmann, J.; Wriedt, M.; Näther, C. Metamagnetism and Single-Chain Magnetic Behavior in a Homospin One-Dimensional Iron(II) Coordination Polymer. *Chem. Eur. J*. **2012**, *18*, 5284−5289.
(25) Suckert, S.; Rams, M.; Böhme, M.; Germann, L. S.; Dinnebier, R. E.; Plass, W.; Werner, J.; Näther, C. Synthesis, structures, magneticand theoretical investigations of Co and Ni coordination polymers with layered thiocyanate networks. *Dalton Trans* **2016**, *45*, 18190−18201.
(26) Suckert, S.; Rams, M.; Germann, L. S.; Cegiełka, D. M.; Dinnebier, R. E.; Näther, C. Thermal Transformation of a Zero-Dimensional Thiocyanate Precursor into a Ferromagnetic Three-Dimensional Coordination Network via a Layered Intermediate. *Cryst. Growth Des.* **2017**, *17*, 3997−4005.
(27) Palion-Gazda, J.; Machura, B.; Lloret, F.; Julve, M. Ferromagnetic Coupling Through the End-to-End Thiocyanate Bridge in Cobalt(II) and Nickel(II) Chains. *Cryst. Growth Des*. **2015**, *15*, 2380-2388 and references therein.
(28) Shurdha, E.; Lapidus, S. H.; Stephens, P. W.; Moore, C. E.; Rheingold, A. L.; Miller, J. S. Extended Network Thiocyanate- and Tetracyanoethanide-Based First-Row Transition Metal Complexes. *Inorg. Chem.* **2012**, *51*, 9655−9665.
(29) Boeckmann, J.; Näther, C. Metamagnetism and Long Range Ordering in μ-1,3 Bridging Transition Metal Thiocyanato Coordination Polymers. *Polyhedron* **2012**, *31*, 587−595.
(30) Shurdha, E.; Moore, C. E.; Rheingold, A. L.; Lapidus, S. H.; Stephens, P. W.; Arif, A. M.; Miller, J. S. First Row Transition Metal(II) Thiocyanate Complexes, and Formation of 1-, 2-, and 3-Dimensional Extended Network Structures of $M(NCS)_2(Solvent)_2$ (M = Cr, Mn, Co) Composition. *Inorg. Chem.* **2013**, *52*, 10583−10594.
(31) Wöhlert, S.; Wriedt, M.; Fic, T.; Tomkowicz, Z.; Haase, W.; Näther, C. Synthesis, Crystal Structure, and Magnetic Properties of the Coordination Polymer $[Fe(NCS)_2(1,2\text{-bis}(4\text{-pyridyl})\text{-ethylene})]_n$ Showing a Two Step Metamagnetic Transition. *Inorg. Chem.* **2013**, *52*, 1061−1068.
(32) Wriedt, M.; Sellmer S.; Näther, C. Coordination polymer changing its magnetic properties and colour by termal decomposition: synthesis, structure and properties of new thiocyanato iron(II) coordination polymers based on 4,4-bipyridine as ligand. *Dalton Trans*. **2009**, 7975–7984.
(33) Wriedt, M.; Jeß, I.; Näther, C. Synthesis, Crystal Structure, and Thermal and Magnetic Properties of New Transition Metal–Pyrazine Coordination Polymers. *Eur. J. Inorg. Chem.* **2009**, 1406–1413.
(34) Zhu, X.; Wang, X-Y.; Li, B.-L.; Wanga, J.; Gao, S. Syntheses, structures and magnetic properties of five iron(II) coordination polymers with flexible bis(imidazole) and bis(triazole) ligands. *Polyhedron* **2012**, *31*, 77–81.
(35) Wöhlert, S.; Runčevski, T.; Dinnebier, R. E.; Ebbinghaus, S. G.; Näther, C. Synthesis, Structures, Polymorphism, and Magnetic Properties of Transition Metal Thiocyanato Coordination Compounds. *Cryst. Growth Des.* **2014**, *14*, 1902−1913.
(36) Yamasaki, M.; Ishida, T. First Iron(II) Spin-crossover Complex with an N_5S Coordination Sphere. *Chem. Lett.* **2015**, *44*, 920–921.
(37) Pohl, K.; Wieghardt, K.; Nuber, B.; Weiss, J. Preparation and Magnetism of the Binuclear Iron(II) Complexes $[\{Fe(C_9H_{21}N_3)X_2\}_2]$ (X = NCS, NCO, or N) and their Reaction with NO. Crystal Structures of $[\{Fe(C_9H_{21}N_3)(NCS)_2\}_2]$ and $[Fe(C_9H_{21}N_3)(NO)(N_3)_2]$. *J. Chem. Soc., Dalton Trans.* **1987**, 187-192.
(38) Bette, M.; Kluge, T.; Schmidt, J.; D. Steinborn, D. Diacetylplatinum(II) Complexes with κ^2-Coordinated Tris(pyridyl)methanol and Tris(pyridyl)methyl Ether Ligands: Structural Insight into the Ligand Dynamics in Solution. *Organometallics* **2013**, *32*, 2216-2227.
(39) Llunell, M.; Casanova, D.; Cirera, J.; Alemany, P.; Alvarez, S. SHAPE (2.1). Continuous Shape Measures calculation. Universitat de Barcelona: Barcelona, Spain, **2013**.
(40) Alvarez, Santiago. Distortion Pathways of Transition Metal Coordination Polyhedra Induced by Chelating Topology. *Chem. Rev.* **2015**, *115*, 13447−13483.
(41) Chilton, N. F.; Anderson, R. P.; Turner, L. D.; Soncini, A.; Murray, K. S. PHI: A powerful new program for the analysis of anisotropic monomeric and exchange-coupled polynuclear *d*- and *f*-block complexes. *J. Comput. Chem.* **2013**, *34*, 1164-1175.
(42) Krzytek, J.; Ozarowski, A.; Telser, J. Multi-frequency, high-field EPR as a powerful tool to accurately determine zero-field splitting in high-spin transition metal coordination complexes. *Coord. Chem. Rev.* **2006**, *250*, 2308-2324.
(43) Monfort, M.; Ribas, J.; Solans, X. Crystal Structures and Ferromagnetic Properties of Two New Dinuclear Complexes with Thiocyanato Bridging Ligands: $\{[Ni_2(1,2\text{-diamino-2-methylpropane})_3(NCS)_2]_2(\mu\text{-}NCS)_2\}[Ni(1,2\text{-diamino-2-methylpropane})_2(NCS)_2].H_2O$ and $[\{Ni_2(1,2\text{-diamino-2-methylpropane})_4\}(\mu\text{-}NCS)_2](PF_6)_2$. Magneto-Structural Correlation. *Inorg. Chem.* **1994**, *33*, 4271-4216.

(44) Bertini, I.; Gatteschi, D.; Scozzofava, A. Single crystal electronic spectra and ligand field parameters of some nickel(II) amine-isothiocyanato and amine-nitrito complexes. *Inorg. Chem.* **1976**, *15*, 203-207.
(45) Oxford Diffraction (2006). Xcalibur CCD/RED CrysAlis Software system. Oxford Diffraction Ltd, Abingdon, England.
(46) Altomare, A.; Burla, M. C.; Camalli, M.; Cascarano, C.; Giacovazzo, C.; Guagliardi, A.; Moliterni, A. G. G.; Polidori, G.; Spagna, R. *SIR*97: a new tool for crystal structure determination and refinement. *J. Appl. Cryst.* **1999**, *32*, 115-119.
(47) Sheldrick, G. Crystal structure refinement with SHELXL. *Acta Cryst. C* **2015**, *71*, 3-8.
(48) Noodleman, L. Valence bond description of antiferromagnetic coupling in transition metal dimers. *J. Chem. Phys*. **1981**, *74*, 5737-43.
(49) Becke, A. D. Density-functional exchange-energy approximation with correct asymptotic behavior. *Phys. Rev. A* **1988**, *38*, 3098–3100.
(50) Lee, C.; Yang, W.; Parr, R. G. Development of the Colle-Salvetti correlation-energy formula into a functional of the electron density. *Phys. Rev. B*, **1988**, *37*, 785-789.
(51) Becke, A. D. Density-functional thermochemistry. III. The role of exact exchange. *J. Chem. Phys,* **1993**, *98*, 5648- 5652.
(52) Frisch, M. J.; Trucks, G. W.; Schlegel, H. B.; Scuseria, G. E.; Robb, M. A.; Cheeseman, J. R.; Montgomery Jr., J. A.; Vreven, T.; Kudin, K. N.; Burant, J. C.; Millam, J. M.; Iyengar, S. S; Tomasi, J.; Barone, V.; Mennucci, B.; Cossi, M.; Scalmani, G.; Rega, N; Petersson, G. A.; Nakatsuji, H.; Hada, M.; Ehara, M.; Toyota, K.; Fukuda, R., Hasegawa, J.; Ishida, M.; Nakajima, T.; Honda, Y.; Kitao, O.; Nakai, H.; Klene, M.; Li, X.; Knox, J. E.; Hratchian, H. P.; Cross, J. B.; Adamo, C.; Jaramillo, J.; Gomperts, R.; Stratmann, R. E.; Yazyev, O.; Austin, A. J.; Cammi, R.; Pomelli, C.; Ochterski, J. W.; Ayala, P. Y.; Morokuma, K.; Voth, G. A.; Salvador, P.; Dannenberg, J. J.; Zakrzewski, V. G.; Dapprich, S.; Daniels, A. D.; Strain, M. C.; Farkas, O.; Malick, D. K.; Rabuck, A. D.; Raghavachari, R.; Foresman, J. B.; Ortiz, J. V.; Cui, Q.; Baboul, A. G.; Clifford, S.; Cioslowski, J.; Stefanov, B. B.; Liu, G.; Liashenko, A.; Piskorz, P.; Komaromi, I.; Martin, R. L.; Fox, D. J.; Keith, T.; Al-Laham, M. A.; Peng, C. Y.; Nanayakkara, A.; Challacombe, M.; Gill, P. M. W.; Johnson, B.; Chen, W.; Wong, M. W.; Gonzalez, C.; Pople, J. A. GAUSSIAN 03 (Revision C.0), Gaussian, Inc., Wallingford, CT, 2004.
(53) Bacskay, G. B. A quadratically convergent Hartree-Fock (QC-SCF) method. Application to closed shell systems. *Chem. Phys.* **1981**, *61*, 385-404.
(54) Schäfer, A.; Hubern C.; Ahlrichs, R. Fully optimized contracted Gaussian basis sets of triple zeta valence quality for atoms Li to Kr. *J. Chem. Phys.* **1994**, *100*, 5829-5835.
(55) Jaguar 7.6, ab initio quantum chemistry package, Schrödinger, Inc., Portland, OR, 2009.
(56) Ruiz, E.; Cano, J.; Alvarez, S.; Alemany, P. Broken symmetry approach to calculation of exchange coupling constants for homobinuclear and heterobinuclear transition metal complexes. *J. Comput. Chem.* **1999**, *20*, 1391–1400.
(57) Ruiz, E.; Alvarez, S.; Rodríguez-Fortea, A.; Alemany, P.; Pouillon Y.; Massobrio C. in Magnetism: Molecules to Materials II: Models and Experiments; Miller, J. S.; Drillon, M, Eds.; Wiley-VCH Verlag GmbH & Co. KGaA, Weinheim, FRG, 2001, Chapter 7, pp 5572.
(58) Ruiz, E.; Rodríguez-Fortea, A.; Cano, J.; Alvarez, S.; Alemany, P. About the calculation of exchange coupling constants in polynuclear transition metal complexes. *J. Comput. Chem*., **2003**, *24*, 982–989.
(59) Ruiz, E.; Alvarez, S.; Cano, J.; Polo, V. About the calculation of exchange coupling constants using density-functional theory: The role of the self-interaction error. *J. Chem. Phys.* **2005**, *123*, 164110.

For Table of Contents Only

A new dinuclear complex [{Fe(tpc-Obn)(NCS)(μ-NCS)}$_2$] (tpc-Obn = tris(2-pyridyl)benzyloxymethane) exhibiting ferromagnetic coupling has been compared to the few previous dinuclear [Fe_2(μ-SCN)$_2$] complexes, exhibiting either ferro-, anti-ferromagnetic or spin crossover (SCO) behavior. The main structural parameters controlling the sign and the magnitude of J_{FeFe} as well as the ligand field energy have been discussed according to detailed magneto-structural studies.